Inorganic Chemistry

Article

pubs.acs.org/IC

Architecture of CuS/PbS Heterojunction Semiconductor Nanowire Arrays for Electrical Switches and Diodes

Xuemin Qian,[†] Huibiao Liu,[†] Nan Chen,[†] Haiqing Zhou,[‡] Lianfeng Sun,[‡] Yongjun Li,[†] and Yuliang Li*[,†]

[†]CAS Key Laboratory of Organic Solids, Beijing National Laboratory for Molecular Sciences (BNLMS), Institute of Chemistry, Chinese Academy of Sciences, Beijing 100190, P. R. China

[‡]National Center for Nanoscience and Technology, Beijing 100190, P. R. China

Supporting Information

ABSTRACT: CuS/PbS p−n heterojunction nanowires arrays have been successfully synthesized. Association of template and DC power sources by controllable electrochemistry processes offers a technique platform to efficiently grow a combined heterojunction nanowire arrays driven by a minimization of interfacial energy. The resulting p−n junction materials of CuS/PbS show highly uniform 1D wire architecture. The single CuS/PbS p−n heterojunction nanowire based devices were fabricated, and their electrical behaviors were investigated. The independent nanowires exhibited a very high ON/OFF ratio of 1195, due to the association effect of electrical switches and diodes.

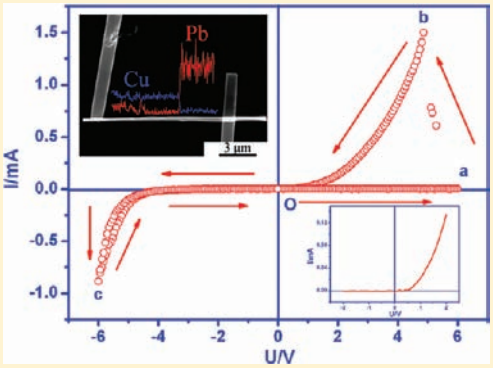

In the past decade, great effort has been devoted to the construction of heterostructured nanowires of semiconductor with modulated compositions which enable the creation of interfaces because of their unique structures and potential application.[1−20] One-dimension (1D) axial heterojunction nanowires provide an opportunity to develop functional materials for use as electronic and photonic devices.[12−32] Achieving finetunability in the optical properties of colloidal nanocrystals is one of the main focuses of research in nanoscience. 1D semiconductor heterostructure interfaces are divided into three categories: inorganic−inorganic,[33−35] inorganic−organic,[36−39] and organic−organic.[40] Most of 1D inorganic−inorganic semiconductor heterojunctions are limited to III−V materials, such as GaAs/GaP[33] and InAs/InP.[34,35] Semiconductor heterojunctions with tunable physical behavior have attracted considerable attention in recent years.[41,42] Among different classes of semiconducting materials, semiconductors of the metal sulfides family are of considerable interest for using as light-emitting diodes, photovoltaic cells, and optical devices. Therefore, systematic tuning of the composition, crystal phase, phase match, size, and shape of metal sulfide semiconducting heterojunctions represents a new field for developing next-generation, low-cost, and high-performance energy and electronic materials. Therefore, the development of highly stable semiconductor heterojunctions especially based on metal sulfides has been a great challenge. A considerable effort has been made to show that metal sulfide, especially Ag_2S/Ag and Cu_2S/Cu, nanofilms are a kind of excellent resistive switching material in previous literature works.[43−45] These nanofilms show similar resistive switching phenomena as well as work mechanism. An interesting phenomenon has been reported that a negative differential resistance (NDR) behavior could be clearly observed in Cu_2S/ZnO p−n heterojunction nanowire array systems at reverse bias,[43] which shows there still is a low resistance state at the beginning of applied voltage turning to reverse range. A similar NDR behavior can be observed in material of Cu_2S/Cu; however, the NDR phenomenon was more obviously due to the rectification effect of the p−n heterojunction. The result indicates that the p−n junction is able to create a large and highly stable ON/OFF ratio nanodevice. In fact, the diode property can be induced to produce the high resistance in the p−n heterojunction nanowire array film and independent nanowire. The high resistance produced can further increase by the diode effect, leading to a very large ON/OFF ratio of an electrical switch, when the p−n heterojunction nanowires possess electrical switch properties. As far as we know, the integration of electrical switches and diodes in p−n heterojunction nanowires has not been reported. In this work, we have successfully constructed the CuS/PbS p−n heterojunction nanowire arrays and studied the electrical switch properties of the independent nanowire. The independent nanowire exhibited a very high ON/OFF ratio of 1195, due to the association effect of the electrical switch and diode on the heterojunction of CuS/PbS wires. The CuS/PbS p−n heterojunction nanowires were first prepared for testing whether the solid heterojunction in the wires can produce the strong junction effect for realizing synergistic ("1 + 1 > 2") performance.

A template with a DC power source by controllable of electrochemistry offers an ideal platform to efficiently organize

Received: March 1, 2012
Published: June 6, 2012

   dx.doi.org/10.1021/ic300471j | *Inorg. Chem.* 2012, 51, 6771−6775

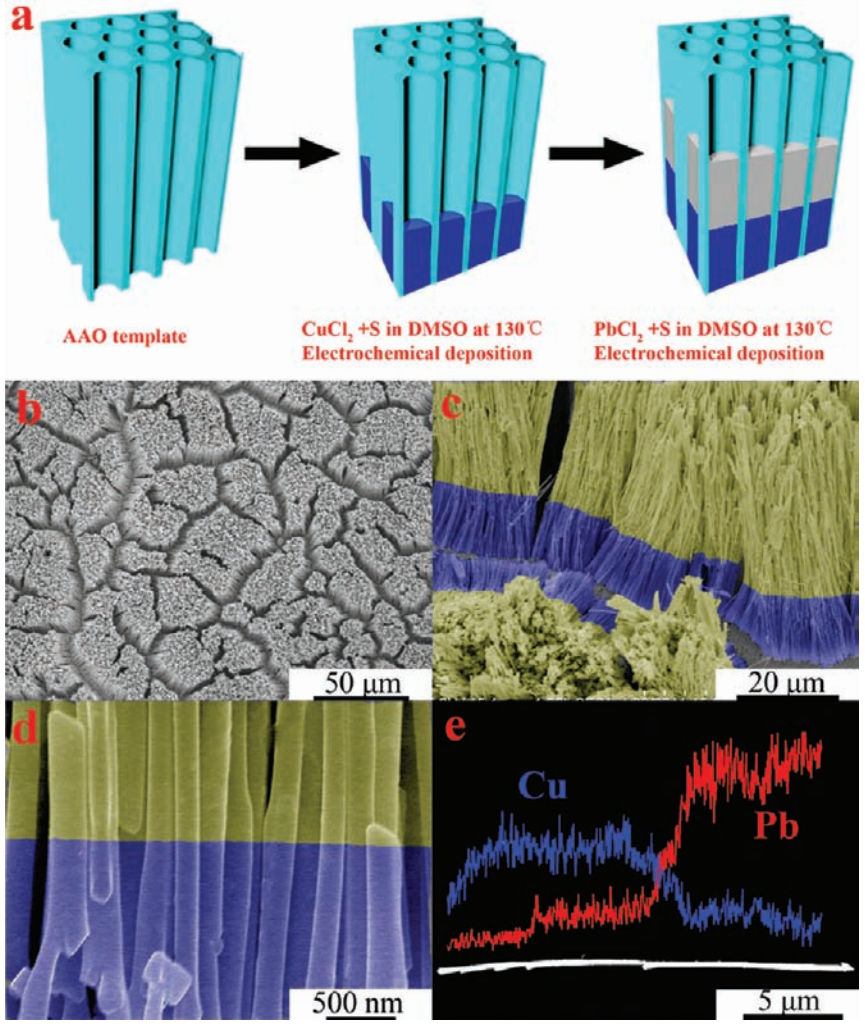

Figure 1. SEM images of CuS/PbS p−n heterojunction nanowires. (a) Scheme of fabricating CuS/PbS p−n heterojunction nanowires. (b) Low magnification top view SEM image. (c) Low magnification side view SEM image. (d) High magnification side view SEM image. (e) Single nanowire SEM image and linear scanning spectrum.

two kinds of nanowires for forming integrative 1D ordered nanowires driven by a minimization of interfacial energy with advantageous optical, electrical, and magnetic properties. This research has been directed toward nanowire hybrids with defined morphologies and showed excellent rectification character at the forward bias and a typical electrical switching properties with large ON/OFF ratios under reverse bias. The assembly route of individual nanowires of PbS and CuS easily creates a homogeneous CuS/PbS p−n junction nanowire. Some elegant studies have been made in synthesizing pure inorganic 1D CuS and PbS nanowires via assembly from corresponding pure CuS and PbS powders. The CuS and PbS are semiconductor that has been used extensively for making thin film and other aggregate structures for electrical conduction,[46] chemical-sensing capabilities,[47] and solar energy absorption.[48] PbS, as a n-type semiconductor, also has been widely used in many fields such as ion-selective sensors,[49] IR detectors,[50] photography,[51] and solar absorbers.[52]

EXPERIMENTAL DETAILS

Synthesis. The CuS/PbS p−n heterojunction nanowires were synthesized by a template-assisted electrodeposition method. A layer of Au was evaporated on the one side of the anodic aluminum oxide (AAO) template as a conducting layer, and the template was put into a homemade electrolytic cell as a working electrode with a platinum counter electrode. CuS nanowires were first deposited into AAO template at a current density of 3.9 mA/cm^2 in a dimethyl sulfoxide (DMSO) solution consisting of 0.05 M $CuCl_2$ and 0.01 M sulfur at 130 °C. After deposition, the template was washed with hot DMSO solution (about 130 °C). Then, PbS nanowires were deposited into the AAO template at a current density of 2.4 mA/cm^2 in a DMSO solution consisted of 0.03 M $PbCl_2$ and 0.01 M sulfur at 130 °C. After the deposition, the AAO templates with the grown nanowires were immediately rinsed with hot DMSO (about 130 °C), then washed with deionized water, and air-dried at room temperature. The CuS/PbS p−n heterojunction nanowires samples were prepared as follows. The AAO templates containing nanowires were pasted on aluminum foil with conductive adhesive. Then, the AAO templates were etched by NaOH solution (2 M) for 30 min at room temperature. After dissolving the template, the nanowires were freed completely standing on the Au layer and washed with deionized water several times and dried in the air.

Characterization. The CuS/PbS p−n heterojunction nanowires were characterized by scanning electron microscopy (SEM, Hitachi S-4800, operated at 15 KV) equipped with an X-ray energy dispersive spectrometer (EDS) and the X-ray diffractometer (XRD, Rigaku Dmax200, Cu Kα). The scanning rate was 0.05°/s, and the 2θ range was from 10° to 80°. The dispersed nanowires were transferred on Cu screen and transmission electron microscopy (TEM) measurements were conducted with JEOL 2010 transmission electron microscopes using an accelerating rate voltage of 200 keV.

dx.doi.org/10.1021/ic300471j | Inorg. Chem. 2012, 51, 6771−6775

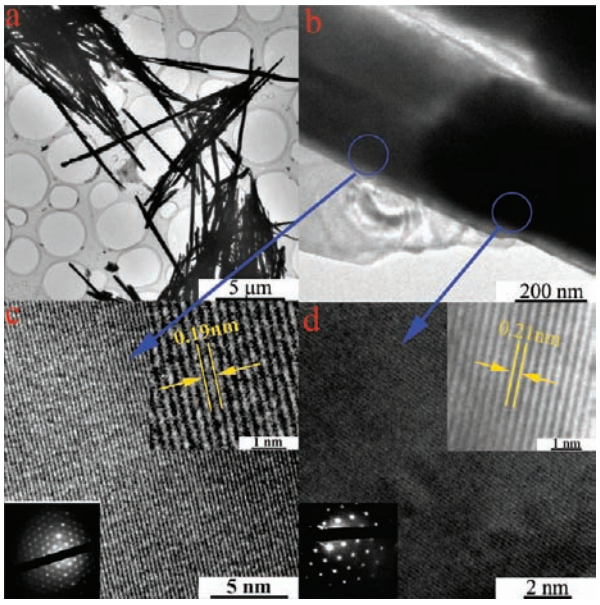

Figure 2. (a) Low magnification TEM image of CuS/PbS p−n heterojunction nanowires. (b) Closeness of CuS/PbS junction. (c) High-resolution TEM image of CuS side: (inset up) large magnification image of HRTEM; (down) the SAED pattern. (d) High resolution TEM image of PbS side: (inset up) large magnification image of HRTEM; (down) the SAED pattern.

Preparation of Nanowire Devices and *I*−*V* Measurements. The single CuS/PbS p−n heterojunction nanowire based devices were prepared as follows. First, the momodisperse CuS/PbS p−n heterojunctions nanowires were transferred onto SiO_2/Si substrate. Then, a layer of photoresist about 100 nm was spinning coated on the substrate. Postprocessing of localization was based on Raiph 150 scanning electron microscopy; the outlines of electrodes were etched by using e-beam technology. After the Cu electrodes were deposited on the ends of the nanowires, the photoresist was washed with acetone. Three single nanowire based devices were fabricated. The experimental *I*−*V* data were recorded with Kethley 4200 semiconductor characteristic system.

RESULT AND DISCUSSION

The as prepared CuS/PbS p−n heterojunction nanowires were characterized by SEM (Figure 1). The top view SEM images show all the nanowires are vertically aligned on the Au foils. The nanowires of CuS side were synthesized with about the length of 10 μm for 60 min (blue side) the part of PbS was synthesized with about the length of 30 μm for 60 min (yellow side). The large magnification SEM image (Figure 1d) shows the nanowires are continuous but the interfaces are not clearly (Supporting Information Figure S1). One single CuS/PbS p−n heterojunction nanowire was characterized by element linear scanning which shows the dispersion of Cu element (blue) and Pb element (red) clearly. The EDS results collected from the heterojunction nanowire display the detailed chemical components, indicating that the heterojunction nanowire was indeed composed of CuS and PbS.

For further investigation, the fine structure of nanowires, CuS/PbS p−n heterojunction nanowires, were characterized by TEM. The low magnification TEM image (Figure 2a) shows that there are numbers of nanowires on the Cu screen. The closeness (Figure 2b) shows that the interface is very flat and the two components contact tightly. Selective area electron diffraction (SAED) was used to characterize the components of

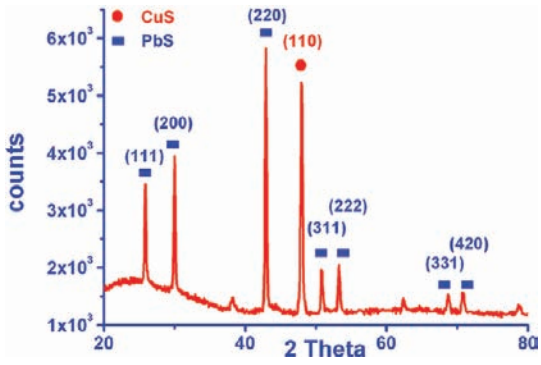

Figure 3. XRD pattern of CuS/PbS p−n heterojunction nanowires.

opposite sides of the interface and showed that both CuS and PbS nanowire are crystalline. The HRTEM images show that the left part of nanowire is composed by CuS with a lattice fringe spacing of 0.19 nm corresponding to the (110) plane of the hexagonal phase of a CuS crystal. The right part of the nanowire is composed by PbS with a lattice fringe spacing of 0.21 nm, corresponding to the (220) plane of the hexagonal phase of a PbS crystal.

The CuS/PbS p−n heterojunction nanowires were characterized by XRD (Figure 3). In this measurement, we removed the AAO templates from the CuS and PbS nanowires arrays to avoid the effect of the AAO templates. The CuS XRD pattern is compared with that of the standard powder diffraction pattern of CuS (JCPDS 79-2321)[53] with hexagonal structure. There is only one strong peak (110) indicating that there was a (110) preferred orientation during the growth of CuS nanowires. We did not observe any phase in the XRD pattern, such as the elemental copper, sulfur, and Cu_2S. The PbS XRD pattern is compared with that of the standard powder diffraction pattern of PbS (ICSD Collection Code 53093)[54] with cubic structure. There are seven peaks, and the intensity of the peak (220) is higher than other peaks, indicating that there was a (220) preferred orientation during the growth of PbS nanowires.

The single CuS/PbS p−n heterojunction nanowire based devices were prepared and their electrical behaviors were investigated. Figure 4a shows one of the three CuS/PbS single nanowire based devices (Supporting Information Figure S2) with two copper electrodes deposited on both ends using e-beam technology. The linear scanning spectrum showed that the nanowire was composed by CuS and PbS. When the bias voltage was applied from −2 to 2 V, the nanowire showed excellent rectification character, and the rectification ratio of the diode was about 44.9 (Figure 4b). When the bias voltage was applied from −6 to 6 V (Figure 4c), the nanowire not only showed excellent rectification character but also showed outstanding electrical switching character. At the beginning, the voltage applied on the PbS side was positive and increased from zero. The current increased slowly through line OA because that the nanowire was under reverse bias. When the applied voltage approached 6 V, point A, the current suddenly increased quickly and a drop in voltage occurred to point B. The electrical switching takes place through line AB. Then, the applied voltage was decreased to zero slowly and the current decreased to zero through line BO. If we define line OA as representing the "OFF" state and line BO representing the "ON" state, the ON/OFF ratio was about 1195 at point B, about 4.86 V. When the voltage applied on the PbS side turned to negative, the nanowire was under forward bias. The applied

dx.doi.org/10.1021/ic300471j | Inorg. Chem. 2012, 51, 6771−6775

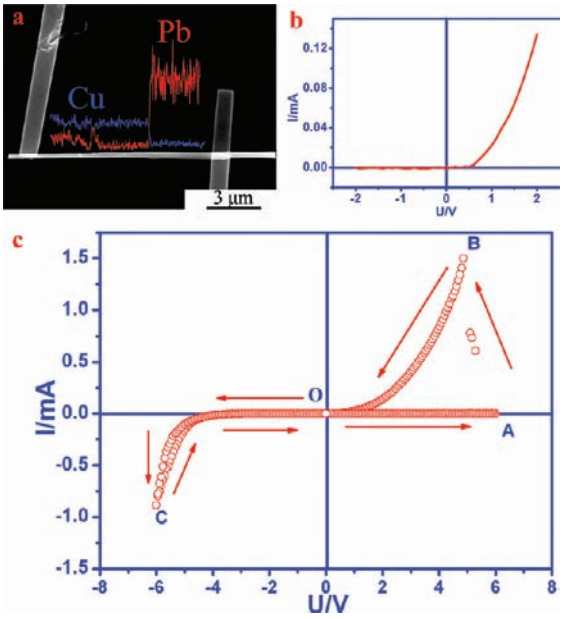

Figure 4. (a) SEM image of a single CuS/PbS p−n heterojunction nanowire. (b) *I*−*V* plot of a single CuS/PbS p−n heterojunction nanowire at the low bias voltage from −2 to 2 V. (c) *I*−*V* plot of single CuS/PbS p−n heterojunction nanowire at the high bias voltage from −6 to 6 V.

voltage decreased from zero to −6 V and then increased to zero. The nanowire showed excellent rectification properties, lines OC and CO. The average rectification ratio of the diode was about 1066. All measurements were repeated three times with the same condition in the same devices, and the results coincided each time. The fact that these results showed such outstanding properties is due to the association effect of electrical switches and diodes on the junction of wires.

The electrical switching behavior of CuS/PbS p−n heterojunction nanowires can be explained as a solid-state electrochemical process (Figure 5).[45] There is an internal electric field (E_{in}) at the interface of CuS and PbS. When the p−n junction was under reverse bias, E_{in} was enhanced which decreased the diffusion of majority carriers. Now, the CuS/PbS device was at the OFF state (with high resistance state) of the switch. At the same time, the Cu^{2+} ions in CuS near the bottom electrode began to be reduced and gradually formed Cu filaments toward the PbS side. And then, the Pb^{2+} ions in PbS were also reduced and formed Pb filaments toward to the top Cu electrode. When the metal bridges directly touched both of the top and bottom electrodes, the CuS/PbS device was at the ON state (with low resistance state) of the switch. The device would be switched off when the applied voltage is swept back, and the metal bridges would break from the metal electrodes.

We also investigated the electrical switching properties of CuS and PbS nanowire based devices. Under the same conditions, the ON/OFF ratios of CuS and PbS nanowires were about 64 and 20 (Supporting Information Figure S3) which were far less than the value of the CuS/PbS p−n heterojunction nanowires. The reason for this should be due to the p−n junction. At the OFF state, the resistance of CuS/PbS nanowire was far larger than those of CuS or PbS nanowires because the p−n junction was under reverse bias. But at the ON state, the resistances of CuS, PbS, and CuS/PbS nanowires were at same magnitude because at this moment only metal bridges provided the resistance. So, the ON/OFF ratio of CuS/PbS nanowires was greatly larger than the values of CuS and PbS nanowires.

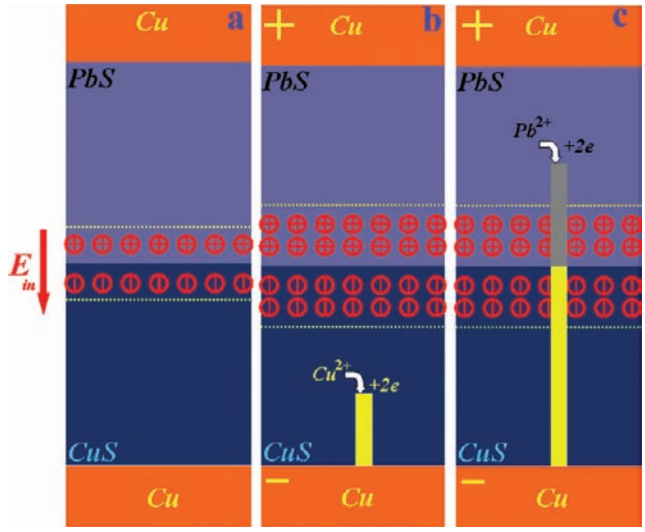

Figure 5. Scheme of the operating mechanism. (a) As-prepared CuS/PbS p−n heterojunction nanowire. (b and c) CuS/PbS p−n heterojunction nanowire under reverse bias.

CONCLUSION

We have successfully synthesized CuS/PbS p−n heterojunction nanowire arrays. The resulting p−n junction materials of CuS/PbS show a highly uniform 1D wire architecture with tunable length and diameter. The nanowires exhibited a very high ON/OFF ratio of 1195, due to the association effect of electrical switches and diodes. Our results provide new insights into the fabrication of new heterojunction structured materials of inorganic semiconductors to achieve properties and functions. The results have confirmed that the p−n junction material of CuS/PbS as produced has distinct properties that were not observed in the individual CuS and PbS, thereby realizing synergistic ("1 + 1 > 2") performance.

ASSOCIATED CONTENT

Supporting Information

Figure S1−S3 as mentioned in the text. This material is available free of charge via the Internet at http://pubs.acs.org.

AUTHOR INFORMATION

Corresponding Author

*E-mail: ylli@iccas.ac.cn.

Notes

The authors declare no competing financial interest.

ACKNOWLEDGMENTS

This work was supported by the National Basic Research 973 Program of China (2011CB932302) and the National Nature Science Foundation of China (21031006, 21021091, and 20831160507).

REFERENCES

(1) Hu, J. Q.; Bando, Y. S.; Golberg, D. J. *Mater. Chem.* **2009**, *19*, 330−343.

(2) Sze, S. M. *Physics of Semiconductor Devices*; Wiley-Interscience: NewYork, 1981.

(3) Mbindyo, J. K. N.; Mallouk, T. E.; Mattzela, J. B.; Kratochvilova, I.; Razavi, B.; Jackson, T. N.; Mayer, T. S. *J. Am. Chem. Soc.* **2002**, *124*, 4020−4026.
(4) Pena, D. J.; Mbindyo, J. K. N.; Carado, A. J.; Mallouk, T. E.; Keating, C. D.; Razavi, B.; Mayer, T. S. *J. Phys. Chem. B* **2002**, *106*, 7458−7462.
(5) Wang, J. G.; Tian, M. L.; Mallouk, T. E.; Chan, M. H. W. *Nano Lett.* **2004**, *4*, 1313−1318.
(6) Martinson, A. B. F.; Elam, J. W.; Hupp, J. T.; Pellin, M. J. *Nano Lett.* **2007**, *7*, 2183−2187.
(7) Hamann, T. W.; Martinson, A. B. E.; Elam, J. W.; Pellin, M. J.; Hupp, J. T. *Adv. Mater.* **2008**, *20*, 1560.
(8) Standridge, S. D.; Schatz, G. C.; Hupp, J. T. *J. Am. Chem. Soc.* **2009**, *131*, 8407.
(9) Song, J. H.; Wang, X. D.; Liu, J.; Liu, H. B.; Li, Y. L.; Wang, Z. L. *Nano Lett.* **2008**, *8*, 203−207.
(10) Pan, Z. W.; Dai, Z. R.; Wang, Z. L. *Science* **2001**, *291*, 1947−1949.
(11) Qian, F.; Li, Y.; Gradecak, S.; Park, H. G.; Dong, Y. J.; Ding, Y.; Wang, Z. L.; Lieber, C. M. *Nat. Mater.* **2008**, *7*, 701−706.
(12) Chen, M. T.; Lu, M. P.; Wu, Y. J.; Song, J. H.; Lee, C. Y.; Lu, M. Y.; Chang, Y. C.; Chou, L. J.; Wang, Z. L.; Chen, L. J. *Nano Lett.* **2010**, *10*, 4387−4393.
(13) Park, S.; Chung, S. W.; Mirkin, C. A. *J. Am. Chem. Soc.* **2004**, *126*, 11772−11773.
(14) Wei, W.; Li, S. Z.; Qin, L. D.; Xue, C.; Millstone, J. E.; Xu, X. Y.; Schatz, G. C.; Mirkin, C. A. *Nano Lett.* **2008**, *8*, 3446−3449.
(15) Wei, W.; Li, S. Z.; Millstone, J. E.; Banholzer, M. J.; Chen, X. D.; Xu, X. Y.; Schatz, G. C.; Mirkin, C. A. *Angew. Chem.Int. Ed.* **2009**, *23*, 4210−4212.
(16) Chen, X. D.; Yeganeh, S.; Qin, L. D.; Li, S. Z.; Xue, C.; Braunschweig, A. B.; Schatz, G. C.; Ratner, M. A.; Mirkin, C. A. *Nano Lett.* **2009**, *9*, 3974−3979.
(17) Chen, X. D.; Zheng, G. F.; Cutler, J. I.; Jang, J. W.; Mirkin, C. A. *Small* **2009**, *5*, 1527−1530.
(18) Zheng, W. Y.; Li, Y. J.; Liu, H. B.; Yin, X. D.; Li, Y. L. *Chem. Soc. Rev.* **2011**, *40*, 4506−4524.
(19) Cui, S.; Liu, H. B.; Gan, L. B.; Li, Y. L.; Zhu, D. B. *Adv. Mater.* **2008**, *20*, 2918−2925.
(20) Liu, H. B.; Cui, S.; Guo, Y. B.; Li, Y. L.; Huang, C. S.; Zuo, Z. C.; Yin, X. D.; Song, Y. L.; Zhu, Z. B. *J. Mat. Chem.* **2009**, *19*, 1031−1036.
(21) Liber, C. M. *Sci. Am.* **2001**, *285*, 58.
(22) Cui, Y.; Lieber, C. M. *Science* **2001**, *291*, 851.
(23) Duan, X. F.; Huang, Y.; Chi, Y.; Wang, J. F.; Lieber, C. M. *Nature* **2001**, *409*, 66.
(24) Cui, Y.; Wei, Q. Q.; Paek, H. K.; Lieber, C. M. *Science* **2001**, *293*, 1289.
(25) Huang, Y.; Duan, X. F.; Cui, Y.; Lieber, C. M. *Science* **2001**, *294*, 1313.
(26) Nirmal, M.; Brus, L. *Acc. Chem. Res.* **1999**, *32*, 407.
(27) Bruchez, M.; Moronne, M.; Gin, P.; Alivisatos, A. P. *Science* **1998**, *281*, 2013.
(28) Liu, H. B.; Xu, J. L.; Li, Y. J.; Li, Y. L. *Acc. Chem. Res.* **2010**, *43*, 1496−1508.
(29) Liu, H. B.; Li, Y. L.; Jiang, L.; Luo, H. Y.; Xiao, S. Q.; Fang, H. J.; Li, H. M; Zhu, D. B.; Yu, D. P.; Xu, J.; Xiang, B. *J. Am. Chem. Soc.* **2002**, *124*, 13370−13371.
(30) Liu, H. B.; Zhao, Q.; Li, Y. L.; Liu, Y; Lu, F. S.; Zhuang, J. P.; Wang, S.; Jiang, L.; Zhu, D. B.; Yu, D. P.; Chi, L. F. *J. Am. Chem. Soc.* **2005**, *127*, 1120−1121.
(31) Gan, H. Y.; Liu, H. B.; Li, Y. J.; Zhao, Q.; Li, Y. L.; Wang, S.; Jiu, T. G.; Wang, N.; He, X. R.; Yu, D. P.; Zhu, D. B. *J. Am. Chem. Soc.* **2005**, *127*, 12452−12453.
(32) Cui, S.; Li, Y. L.; Guo, Y. B.; Liu, H. B.; Song, Y. L.; Xu, J. L.; Lv, J.; Zhu, M.; Zhu, D. B. *Adv. Mater.* **2008**, *20*, 309−313.
(33) Gudiksen, M. S.; Lauhon, L. J.; Wang, J.; Smith, D. C.; Lieber, C. M. *Nature* **2002**, *415*, 617.
(34) Bjork, M. T.; Ohlsson, B. J.; Sass, T.; Persson, A. I.; Thelander, C.; Magnusson, M. H.; Deppert, K.; Wallenberg, L. R.; Samuelson, L. *Appl. Phys. Lett.* **2002**, *80*, 1058.
(35) Bjork, M. T.; Ohlsson, B. J.; Sass, T.; Persson, A. I.; Thelander, C.; Magnusson, K.; Deppert, M. H.; Wallenberg, L. R.; Samuelson, L. *Nano Lett.* **2002**, *2*, 87.
(36) Guo, Y. B.; Tang, Q. X.; Liu, H. B.; Zhang, Y. J.; Li, Y. L.; Hu, W. P.; Wang, S.; Zhu, D. B. *J. Am. Chem. Soc.* **2008**, *130*, 9198−9199.
(37) Guo, Y. B.; Liu, H. B.; Li, Y. J.; Li, G. X.; Zhao, Y. J.; Song, Y. L.; Li, Y. L. *J. Phys. Chem. C.* **2009**, *113*, 12669−12673.
(38) Lin, H. W.; Liu, H. B.; Qian, X. M.; Lai, S. W.; Li, Y. J.; Chen, N.; Ouyan, C. B.; Che, C. M.; Li, Y. L. *Inorg. Chem.* **2011**, *50*, 7749−7753.
(39) Chen, N.; Qian, X. M.; Lin, H. W.; Liu, H. B.; Li, Y. J.; Li, Y. L. *Dalton Trans.* **2011**, *40*, 10804−10808.
(40) Guo, Y. B.; Zhang, Y. J.; Liu, H. B.; Lai, S. W.; Li, Y. L.; Li, Y. J.; Hu, W. P.; Wang, S.; Che, C. M.; Zhu, D. B. *J. Phys. Chem. Lett.* **2010**, *1*, 327−330.
(41) Ren, Y.; Chiam, S. Y.; Chim, W. K. *Nanotechnology* **2011**, *22*, 235606.
(42) Mattias Borg, B.; Martin, E. K.; Dick, K. A.; Ganjipour, B.; Dey, A. W.; Thelander, C.; Wernersson, L. *Appl. Phys. Lett.* **2011**, *99*, 203101.
(43) Liu, X. H.; Mayer, M. T.; Wang, D. W. *Appl. Phys. Lett.* **2010**, *96*, 223103.
(44) Sakamoto, T.; Sunamura, H.; Kawaura, H. *Appl. Phys. Lett.* **2003**, *82*, 3032−3034.
(45) Wang, H. L.; Qi, L. M. *Adv. Func. Mater* **2008**, *18*, 1249−1256.
(46) Mane, R. S.; Lokhande, C. D. *Mater. Chem. Phys.* **2000**, *65*, 1.
(47) Janata, J.; Josowicz, M.; DeVaney, D. M. *Anal. Chem.* **1994**, *66*, R207.
(48) Liao, X. H.; Chen, N. Y.; Xu, S.; Yang, S. B.; Zhu, J. J. *J. Cryst. Growth* **2003**, *252*, 593.
(49) Chaudhur, T. K.; Chatterjes, S. *Proc. Int. Conf. Thermoelectr.* **1992**, *11*, 40.
(50) Nair, P. K.; omezdaza, O. G.; M. Nair, T. S. *Adv. Mater. Opt. Electron.* **1992**, *1*, 139.
(51) Gadenne, P.; Yagil, Y.; Deutscher, G. *J. Appl. Phys.* **1989**, *66*, 3019.
(52) Hirata, H.; Higashiyama, K. *Bull. Chem. Soc. JPN.* **1971**, *44*, 2420.
(53) Wu, C.; Shi, J. B.; Chen, C. J.; Lin, J. Y. *Mater. Lett.* **2008**, *62*, 1074−1077.
(54) Wu, C.; Shi, J. B.; Chen, C. J.; Wei, S. Y. *Mater. Lett.* **2006**, *60*, 3618−3621.